CHEMICAL ENGINEERING TRANSACTIONS
VOL. 96, 2022
A publication of AIDIC
The Italian Association of Chemical Engineering
Online at www.cetjournal.it
Guest Editors: David Bogle, Flavio Manenti, Piero Salatino

ISBN 978-88-95608-95-2; **ISSN** 2283-9216
DOI: 10.3303/CET2296014

Evaluation of Electrosorption Process for Phosphate and Nitrate Removal from Wastewater

Shreenath Krishnamurthy[a]*, Kaushik Jayasayee[b], Tom-Andre Enebakk Eide[b], Katie McKay[b], Roman Tschentscher[a], Ruth Elisabeth Stensrød[a],Martin Fleissner Sundig[c]

[a] Process Technology, SINTEF Industry, Forskningsveien 1 Oslo 0373, Norway
[b] Sustainable Energy Technology, SINTEF Industry, Sem Sælands vei 12. 7034, Trondheim, Norway
[c] Sustainable Energy Technology, SINTEF Industry, Forskningsveien 1 Oslo 0373, Norway

The present work is dedicated to the preparation and characterization of carbon-based electrodes for the removal of phosphates and nitrate ions from wastewater by CDI method. Carbons obtained from the pyrolysis were used to prepare electrodes and these electrodes were characterized using a number of experimental techniques. Based on the experimental results, the electrodes showed a strong affinity towards the nitrates than phosphates. This was evident from the kinetic constants and significantly higher capacity of electrosorption. At 1mM solutions, representative of a typical wastewater, nitrate exhibited about 3.5 times higher concentration than phosphates on a molar basis. The electrodes were reasonably stable under low concentrations of nitrates. At higher concentrations, the electrodes were not completely regenerable when the desorption step was carried out at 0V. These results are covered in this manuscript.
Keywords: CDI, Electrosorption, wastewater, cyclic voltammetry.

1. Introduction

Capacitative deionization (CDI) is a technique that is gaining widespread attention for removal of ionic contaminants from wastewater [Porada et al., 2013, Tang et al., 2015]. In this process, electrodes are charged and discharged in a cyclic manner. When the electrodes are charged, ions from solution migrate towards the electrode and form an electric double layer (EDL) at the liquid-solid interface. By applying a reverse polarity/shorting/applying no potential, the ions are discharged from the electrode, thereby, leaving no secondary waste. Activated carbon is a well-known material in the wastewater treatment industry and it is a commercially available sorbent made from a variety of sources like plant wastes, coal, and plastics. Activated carbon also has excellent electrical properties, and therefore is an excellent choice of material for electrodes for capacitative deionization [Zhao et al., 2012].
The aim of this work is to characterize electrodes for electrosorption of phosphates and nitrates. The electrodes were prepared using biochar obtained from European red pine, Pinus Sylvestris. Batch experiments were carried out at different phosphate and nitrate concentrations to study adsorption equilibrium and kinetics. The experiments were carried out for different voltages up to 1V to identify the effect of the voltage on the adsorption equilibrium. Further stability tests were carried out to identify the cyclic performance of the electrodes.

2. Materials and methods

2.1. Preparation of electrolyte solutions

Ammonium nitrate (NH_4NO_3) (>99% pure) and potassium phosphate monobasic (KH_2PO_4) solutions (>99% pure) were obtained from Merck and Sigma Aldrich, respectively. 250 ml solutions of the electrolytes at varying concentrations were prepared by dissolving the appropriate amount of the salt (for example 20 mg in 250 ml for NH_4NO_3) in distilled water. The solutions were stirred overnight using a magnetic stirrer (Heidoph MR 3002 C) prior to the experiments. The commercial activated carbon used in these experiments were purchased from Merck (Lot number 1.02184.1000).

Paper Received: 12 December 2021; Revised: 18 June 2022; Accepted: 4 August 2022
Please cite this article as: Krishnamurthy S., Jayasayee K., Enebakk Eide T.A., Mckay K., Tschentscher R., Stensrod R.E., Fleissner Sundig M., 2022, Evaluation of Electrosorption Process for Phosphate and Nitrate Removal from Wastewater, Chemical Engineering Transactions, 96, 79-84 DOI:10.3303/CET2296014

Carbon from pine wood was obtained through pyrolysis of the wood chips at 700℃, for 1.5 hours in CO_2 atmosphere. More details about the pyrolysis are described in an earlier publication [Kalayani et al., 2017].

2.2 Electrode preparation

The stainless-steel substrates were pre-polished and cleaned using a solvent mixture containing DI water and isopropyl alcohol in an ultrasonic bath prior to coating with the carbon ink using a hand spray gun. Usual an ink based for two electrodes at a time were made of 100 mg carbon, 180 mg fumion solution and thinned out with a 50/50 ratio of DI water and iso propyl alcohol, receiving 2.6% solids in liquid. The ink was then ultrasonicated for 15 minutes in sequences of 5 minutes, and stirred for an hour before pipetted out from a suspension and spray coated to a preheated substrate of 55-65°C. After spray coating the sample was left drying while substrate cooled for approximately 15 minutes. To calculate carbon loading on the stainless-steel substrate it was weighed prior and after spray coating. The final electrode contained about 2 mg of carbon/cm².

2.3 Cyclic voltammetry

A three-electrode electrochemical cell from Gaskatel was used to record the cyclic voltammograms (CV) of the carbon-based electrodes. Different concentrations (10 mM, 100mM, 1000 mM) of NH_4NO_3 and (1 mM, 100 mM, and 1000 mM) KH_2PO_4 solutions were prepared. CV tests were performed by cyclic the voltage and measuring the resultant current. For the CV tests, different scan rates of 10, 20, 30, 40 and 50mV/s were used. About 2 cm^2 of the electrode was exposed to the electrolyte.

2.4 X-ray photoelectron spectroscopy (XPS)

XPS measurements were carried out to study the electrode material after adsorption. They were carried out using an AxisUltra^{DLD} XP spectrometer from Kratos Analytical using monochromatic Al Kα radiation (hv=1486.6 eV). The analysis area is approximately 700 x 300 μm^2. The resolution is 1.2 eV for the settings used for the survey spectra and 0.7 eV for the detail spectra, as determined by the full width at half maximum of the Ag $3d_{5/2}$ peak obtained on sputter cleaned silver. The energy scale was referenced based on the position of the C 1s peak from C-C/C-H bonds, set to 284.8 eV binding energy (BE), and quantification is based on the manufacturer's relative sensitivity factors. The analysis was carried out on the used and the unused parts of the electrode.

2.5 Batch tests

The batch test apparatus is a simple set up shown in Figure 1. It is made up of a beaker which contains the electrolyte of known concentration, the working electrode, counter electrode, and the reference electrode all of which are connected to the potentiostat. The working electrode and the counter electrode are made up of carbon coated onto a stainless-steel substrate. The thickness of the electrodes is approximately 0.5 mm. The reference electrode is made up of Ag/AgCl (Metrohm).

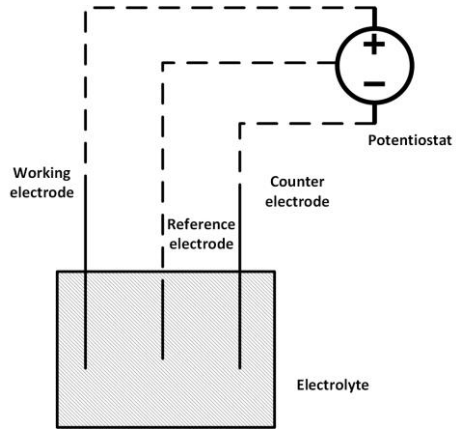

Figure 1: Schematic of the batch setup used in this study.

The experiment consists of two steps, adsorption in which a known potential is applied and desorption where the potential across the two electrodes is set to 0. The experiment is begun by applying a known potential across the electrode at time t=0.The desorption step is performed by switching the voltage to 0V and in this step the ions migrate from the electrode surface to the solution.

The experiments were carried out for 5 different voltages namely 0.2 V, 0.4V, 0.6V, 0.8V and 1V for four different concentrations of 1 mM, 10 mM, 100 mM and 1M electrolyte solutions for NH_4NO_3 and 0.1 mM, 1 mM, and 10 mM solutions for KH_2PO4 for the electrodes made from both carbon sources. The experiments were carried out by starting at the lowest voltage and increasing the voltage in steps of 0.2 V to 1V. The maximum voltage was fixed to 1V in order to avoid any current overload in the system and potentially to avoid being closer to 1.2V where faradaic reactions can occur.
The amount adsorbed is obtained by integrating the transient current response with respect to time given by the equation below:

$$\text{Amount adsorbed} = \frac{\text{MW}_{\text{SALT}}}{\text{FM}_{\text{carbon}}} \int_0^t \text{I(t)dt} \quad (1)$$

Here, F is the faraday Constant (96485.33 C/mol), MW_{SALT} is the molecular weight of the salt and M_{carbon} is the amount of carbon deposited in the working electrode. The amount adsorbed is expressed in mg/g.
The transient responses were also used to study the adsorption kinetics by fitting the responses to a pseudo first order kinetics and a pseudo second order kinetics equation. The expression for the 1st order and 2nd order rate equation are as follows:

$$q(\text{t}) = \left(1 - \text{e}^{-\text{k}_1\text{t}}\right)\text{q}_\text{e} \quad (2)$$

$$q(t) = \frac{q_e k_2 t}{1 + k_2 t} \quad (3)$$

Where, q_e is the concentration at equilibrium (mg/g), k_1 and k_2 are the pseudo 1st and 2nd order rate constants in (s^{-1}), respectively and t is the time in seconds.

3. Results and discussion

3.1 Cyclic voltammetry

Figure 4 shows the current vs voltage curves for 1 mM NH_4NO_3 solution at different scan rates. The current is reported in milliamperes, and the voltage is in volts. The capacitance is defined as

$$Capacitance\ C = \frac{Charge}{Voltage \times mass\ of\ carbon} = \frac{Current}{scan\ rate \times mass\ of\ carbon} \quad (4)$$

The above equation was used to calculate the capacitance in Farad/gram (F/g) by dividing the current in the y axis of figure by the scan rate. The mass of carbon used in the experiments was about 4 mg. One can see from Figure 2 that the capacitance is lower as the scan rate is increased. The capacitance values for the different electrolyte concentrations are shown in Figure 2. The capacitance values are 7, 13 and 18 F/g for 1, 100 and 1000 mM NH_4NO_3 solutions. These are close to the values reported by Pastushok et al [Pastushok et al., 2019]. The values are lower for phosphates and compared to that of nitrates. For phosphates, the values are lower than the ones reported in literature and could be due to the differences in the type of the electrolyte as well as the method of the preparation of the electrode [Huang et al., 2014, Chen et al., 2020]. The capacitance values of phosphates at concentrations < 10 mM are not shown here. This is due to the significant resistance observed during the measurements at these concentrations, which could have led to erroneous values in the capacitance.

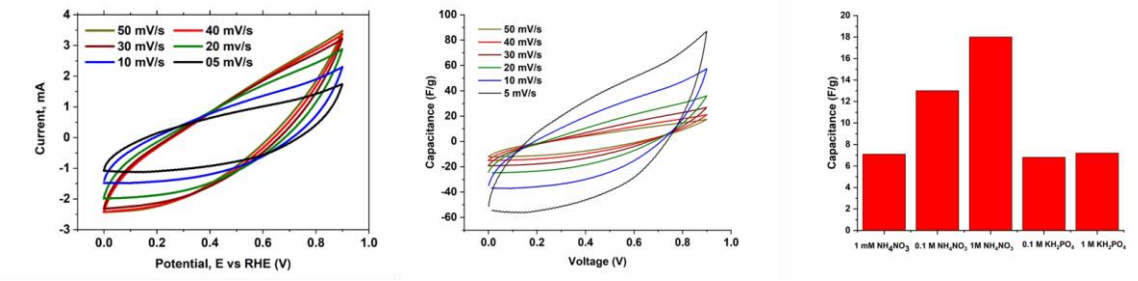

Figure 2: Potential vs current (Left), capacitance vs voltage (Middle) and capacitance vs concentration (Right)

3.2 Batch tests

3.2.1 Adsorption equilibrium

Integrating the area under the transient current curve provided the capacity of the nitrate and the phosphate ions adsorbed in the electrode. The adsorption capacity of the nitrates (NO_3^-) was higher than that of the phosphate ions ($H_2PO_4^-$) and this is consistent with the findings of Macias et al [Macias et al., 2014]. Nitrate ion has a radius of 0.3 nm and the $H_2PO_4^-$ ion has a radius of 0.45 nm. The smaller nitrate ion would be more energetically favourable for adsorption and hence the adsorption capacity is higher.

Table 1 summarizes the adsorption capacity for the different ions at different concentrations. One can clearly see that with an increase in concentration of the electrolyte, the adsorption capacity increases. This is consistent as an increased concentration in the solution would improve the driving force for the adsorption. In our work, we did not saturate the electrodes prior to the experiments and therefore the total capacity is probably that of the physisorption and electrosorption. Further, most of the experiments are based on flow cells in which a known concentration of electrolyte is introduced to the electrodes at known flowrates. The capacity is then calculated by integrating the transient concentration curve which may not be up to completion. This could primarily be the reason for the higher capacity reported in this work than what is observed in literature for nitrates and phosphate adsorption.

Table 1: Capacity values for different NH_4NO_3 and KH_2PO_4 solutions.

Electrolyte	Concentration	Capacity (mol/kg)	Capacity (mg/g)
NH_4NO_3	0.4 mM	0.28	22.25
	1 mM	1.43	114.14
	10 mM	2.02	161.6
	100 mM	3.76	301.14
	1 M	5.43	434.35
KH_2PO_4	0.2 mM	0.08	11.09
	1 mM	0.11	14.7
	10 mM	0.14	18.4

3.2.2.Electrosorption kinetics

The transient response of the current in the working electrode was first normalised based on the initial and final values of current. The normalised current value is a representation of the approach to the equilibrium adsorption capacity in the following manner:

$$q(t) = 1 - \frac{I(t) - I_{min}}{I_{max} - I_{min}} \quad (4)$$

The resultant curves were fitted to the pseudo first order and second order kinetics equations for nitrate and phosphate. It can be seen that the pseudo second order model describes the adsorption well. The kinetic constant k_2 increases with an increase in the concentration of nitrates and phosphates. This agrees with the transient response, where the adsorption is faster (i.e., the baseline is reached faster) at higher concentrations. A comparison between experiments and the model are provided in Figure 3.

3.2.3 Stability

Once the 1V experiments were complete, experiments were repeated first at 0.6V for 4 different cycles to study the capacity change with respect to repeated operation. These experiments were carried out after the 1V experiment, and the capacity values are provided in Figure for 1mM solutions of NH_4NO3 and KH_2PO_4. When experiments were carried out after the 1V experiment the drop in capacities were significant (16 vs 11.9 mg/g) for the 1st run and with respect to subsequent run the drop in capacity was around 10% The drop in capacity with respect to run 1 and run 2 was nearly 70% and the capacity did not change much with subsequent runs. In this scenario, the durations of the adsorption and desorption steps were kept constant.

In this work we have also studied the reuse of the electrodes that were exposed to higher electrolyte concentrations of 100 mM and 1 M Solutions. These electrodes were tested again with 1 mM NH_4NO_3 solution. In this case, the capacity dropped to 97 mg/g as opposed to 114 mg/g with respect to the pristine electrode and it could be that complete removal of the nitrate ions was not possible during the desorption step. The loss in capacity can be attributed to the desorption step being operated at 0 V. one may recommend switching to lower voltages for complete removal of ions.

To understand this XPS acquisitions (Figure 4) were taken on the used and unused parts of the electrode to analyse the nitrogen content and chemistry. Three peaks from different nitrogen species can be discerned in the XP spectra, at binding energies typical, but not exclusive, for -NH_2 bonds (400.0 ±0.3 eV BE), -NH_3^+ bonds (402.4 ±0.3 eV BE) and -NO_2 or -ONO_2 groups (406.4 ±0.3 eV BE), both in the used and unused areas (figure. 4) [Beisinger M, NIST XPS data base, Hantsche 1993]. The proportion of the three nitrogen species differs, however, notably between the areas of the electrode: the concentration of the component at ~402.4 eV BE remains roughly constant while the content of both the low and high binding energy components increases notably in the used area. This would mean that there is still residual nitrate left in the electrode which caused a loss in the capacity. The NH_2 and other nitrogen containing groups may come from the fumion binder. Table 2 summarizes the area under the peaks for used and unused electrodes.

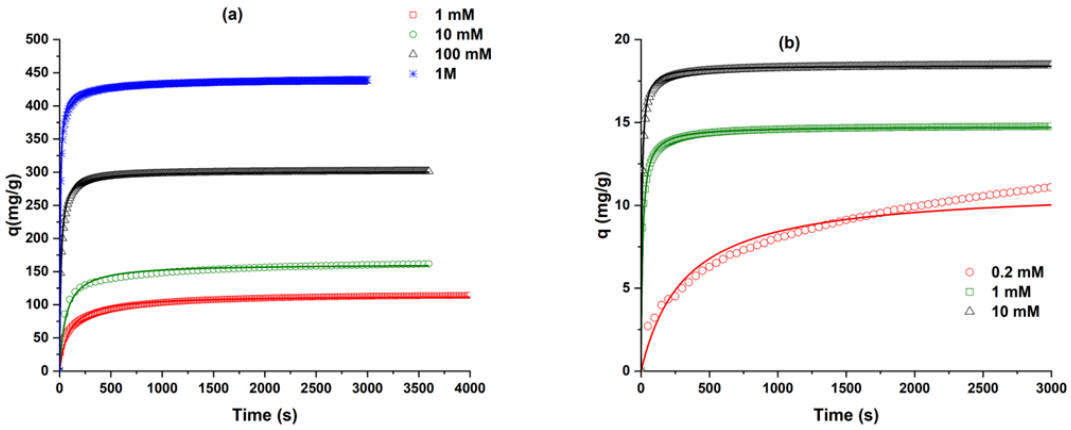

Figure 3: Capacity vs time for the different concentrations (a) NH_4NO_3 and (b) KH_2PO_4. Symbols denote experiments while line is the 2nd order model fit.

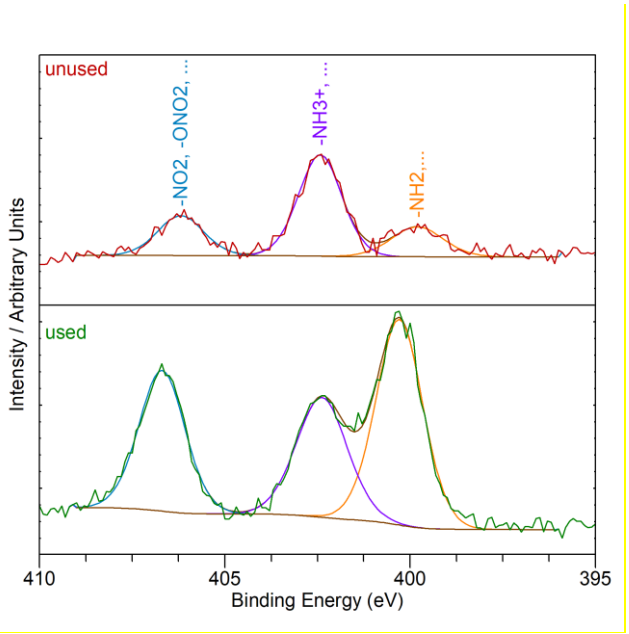

Figure 4: XPS spectra for used and unused electrodes.

Table 2: Area under the curve for different XPS spectra.

-Type	-NH_2, ...	-NH_3^+, ...	-NO_2, -ONO_2, ...
	400.0 ±0.3 eV BE	402.4 ±0.3 eV BE	406.4 ±0.3 eV BE
Used	0.4	1.1	0.5
Unused	2.2	1.4	1.5

4. Conclusions

This work is just a basic step to characterize electrodes in the context of CDI process for nitrate and phosphate removal. The electrodes prepared by spray coating a carbon paint on a stainless-steel substrate showed good affinity for phosphate and nitrate removal. However, stability with at higher concentrations is a serious challenge and based on our preliminary studies, the CDI process is more suited for the low concentration system of less than 1mM solutions for phosphate and nitrate removal. Further, more the understanding of the electrode performance under a real scenario in the presence of other ions like Cl^-, Ag+ Cu^{2+} etc is needed. Also, the electrodes needed to be studied under flow conditions to evaluate the separation potential of these electrodes. Nevertheless, the characterization will serve as an important input for the technical and economic evaluation of the CDI process which would be reported in a further study.

Acknowledgement

This work is a part of the SINTEF's internally funded project, ELEPHONT. The authors would also like to thank several people from the CDI community (Dr Biesheuvel of Wetsus, Prof Dutta of KTH Stockholm, Dr Steven Hand of Carollo Engineers and Tristan Hasseler of Stanford University) for helping us out with their valuable inputs.

References

Biesinger, M. X-ray Photoelectron Spectroscopy (XPS) Reference Pages.

Chen, F.-F., et al., Characteristic and model of phosphate adsorption by activated carbon electrodes in capacitive deionization. Separation and Purification Technology, 2020. 236: p. 116285.

Hantsche, H., High resolution XPS of organic polymers, the scienta ESCA300 database. By G. Beamson and D. Briggs, Wiley, Chichester 1992, 295 pp., hardcover, £ 65.00, ISBN 0-471-93592-1. Advanced Materials, 1993. 5(10): p. 778-778.

Huang, G.-H., et al., Capacitive deionization (CDI) for removal of phosphate from aqueous solution. Desalination and Water Treatment, 2014. 52(4-6): p. 759-765.

Kalyani, D.C., et al., Valorisation of woody biomass by combining enzymatic saccharification and pyrolysis. Green Chemistry, 2017. 19(14): p. 3302-3312.

Macías, C., et al., Improved electro-assisted removal of phosphates and nitrates using mesoporous carbon aerogels with controlled porosity. Journal of Applied Electrochemistry, 2014. 44(8): p. 963-976.

NIST X-ray Photoelectron Spectroscopy Database.

Pastushok, O., et al., Nitrate removal and recovery by capacitive deionization (CDI). Chemical Engineering Journal, 2019. 375: p. 121943.

Porada, S., et al., Review on the science and technology of water desalination by capacitive deionization. Progress in Materials Science, 2013. 58(8): p. 1388-1442.

Tang, W., et al., Fluoride and nitrate removal from brackish groundwaters by batch-mode capacitive deionization. Water Research, 2015. 84: p. 342-349.

Zhao, R., et al., Time-dependent ion selectivity in capacitive charging of porous electrodes. Journal of Colloid and Interface Science, 2012. 384(1): p. 38-44.